Monodisperse Colloidal Silica Spheres from Tetraalkoxysilanes: Particle Formation and Growth Mechanism

A. VAN BLAADEREN,[1] J. VAN GEEST, AND A. VRIJ

Van't Hoff Laboratory, University of Utrecht, Padualaan 8, 3584 CH Utrecht, The Netherlands

Received March 10, 1992; accepted May 19, 1992

The mechanisms behind the formation and growth of silica particles prepared from tetraalkoxysilanes in alcoholic solutions of water and ammonia were investigated. By analyzing the competitive growth of a dispersion of silica spheres with a bimodal size distribution, it was established that the growth proceeds through a surface reaction-limited condensation of hydrolyzed monomers or small oligomers. By following the hydrolysis of tetraethoxysilane with ^{13}C liquid NMR and the particle growth with time-resolved static light scattering, it was found that both processes were described by the same first-order rate constants. Therefore, despite the fact that the incorporation of hydrolyzed monomers proceeds through a reaction-limited process, the overall rate of the particle growth is limited by the first-order hydrolysis rate of the alkoxide. It was concluded that the particle formation (or particle nucleation) proceeds through an aggregation process of siloxane substructures that is influenced strongly by the surface potential of the silica particles and the ionic strength of the reaction medium. These conclusions were based on the dependence of the particle stability and final particle size on additions of $LiNO_3$ to the reaction and dispersion medium and the independence of the growth rate on the same additions.

I. INTRODUCTION

Monodisperse colloidal silica spheres can be prepared by a simple procedure from tetraalkoxysilanes in alcoholic solutions:

$$Si(OC_2H_5)_4 + 4H_2O \xrightarrow[\text{alcohol}]{NH_3} Si(OH)_4 + 4C_2H_5OH \quad [1]$$

$$Si(OH)_4 \xrightarrow[\text{alcohol}]{NH_3} SiO_2\downarrow + 2H_2O. \quad [2]$$

Hydrolysis, Eq. [1], and condensation, Eq. [2], of the monomers (in this paper only tetraethoxysilane, TES, is used) are base-catalyzed by ammonia, which also provides the particles with a negative, stabilizing surface charge. Stöber *et al.* (1a) recognized the importance of the synthesis of monodisperse spherical particles when they investigated the experimental conditions that led to the formation of uniform, spherical silica particles as observed earlier by Kolbe (1b). It appeared possible to produce silica spheres with radii from 10 to 500 nm, covering almost the entire colloidal size range. The reaction parameters were further studied in detail by Van Helden *et al.* (2) and subsequently by Bogush *et al.* (3).

Despite many investigations in which silica spheres prepared from alkoxysilanes have been used as model particles, it is only recently that research has been aimed at elucidating the mechanisms behind the formation and growth of the particles (5–17). A general agreement on the processes responsible for the particle formation and growth, final monodispersity, particle size, and shape has not yet emerged. Differences that are found in the literature are best illustrated by two extremes.

Matsoukas and Gulari (8–10) model particle formation and growth solely by kinetic equations that describe chemical reactions. In their model particle nucleation is the result of the reaction between two reactive, i.e., hydro-

[1] To whom correspondence should be addressed.

0021-9797/92 $5.00

lyzed, monomers. Subsequently, the "particle" grows only by monomer addition. The balance between monomer addition and nucleation determines the polydispersity and final particle size. Particle growth is rate-limited by the slowest step, the hydrolysis of the monomers.

Zukoski and co-workers (11–14) model nucleation and growth by a controlled aggregation mechanism of subparticles a few nanometers in size. Zukoski and co-workers assume that hydrolysis is not the rate-determining step in the particle growth, but that some step in the condensation pathway is rate-determining. Particle formation results from the aggregation of subparticles that are slowly produced during the entire reaction period. This aggregation process is controlled in the sense that once the aggregates or "particles" have reached a certain size (and thereby a certain colloidal stability because of their surface charge), the growth continues only by aggregation with the small subparticles and not by collisions with other (larger) particles. Growth, final particle size, and polydispersity are influenced in this model by parameters like the surface charge and the size of the subparticles.

In a previous paper (17) we investigated the influence of the chemical microstructure on the particle morphology. The microstructure was determined with solid-state ^{13}C and ^{29}Si nuclear magnetic resonance spectroscopy (NMR). It was found that the siloxane structure of all the silica particles investigated was close to 60% Q^4, 35% Q^3, and several percent Q^2, and that several percent of the ethoxy groups never leave the TES molecules. Thus, the separate steps as represented by Eqs. [1] and [2] are an oversimplification. No relation was found between the particle morphology (surface roughness, particle shape) and the chemical microstructure. It was proposed, that an irregular particle shape and a rough surface were the result of "building units" composed of larger siloxane structures, whereas smooth, spherical particles were the result of building units of (much) smaller size: monomers and small oligomers.

In this paper we describe measurements on the kinetics of the particle growth, the hydrolysis of the monomers, and the particle formation (or nucleation). Hydrolysis of TES was followed by ^{13}C NMR and is compared with measurements of the particle growth made with time-resolved static light scattering. It is shown that the condensation on the particle surface occurs through a reaction-limited process, whereas the particle growth rate is limited by the hydrolysis of the monomers. The local particle growth mechanism (as opposed to the rate of the overall particle growth) is demonstrated by using the technique of competitive growth as developed earlier by Bradford *et al.* (18) for latex dispersions. In this technique the relative distance of the two peaks in a bimodal distribution of particles is followed as a function of the particle size with transmission electron microscopy (TEM).

It was further shown by us (5) that the final particle size is influenced strongly by the ionic strength of the reaction medium. Here, we show that it is also strongly influenced by the concentration of ammonia and water. This can be understood from a proposed mechanism in which the final particle size is strongly dependent on the stability of the (intermediate) particles.

This paper is further organized as follows: In Section II a brief literature survey of the experimental techniques used to study formation and growth is given and the mechanisms for explaining the experimental results are presented. Subsequently, the theory behind the competitive growth technique and the particle growth as measured with static light scattering is briefly explained. (Theory on the hydrolysis and condensation of alkoxysilanes is described in previous papers and references therein (17).) After an experimental section (III), particle stability measurements and the kinetics of growth and hydrolysis are discussed (Section IV). Finally, in Section V the experimental data are summarized and interpreted within a proposed formation and growth mechanism.

II. THEORY

A. Previous Work

This brief overview is not organized chronologically, but starts with the work of Matsoukas and Gulari and Zukoski and co-workers, who have done the most work on developing a theoretical framework to explain their experimental findings. As already mentioned in the Introduction, the theories put forward by these two groups contain a number of important differences.

Matsoukas and Gulari (8) measured the particle mass by measuring the scattered intensity. The particle mass as a function of time was found to be described by a single exponential. By measuring the intensities of the bonds of ethoxy groups bound to TES and to free ethanol by Raman spectroscopy, the hydrolysis could be followed as a function of time as well. It was found that the first-order rate constant of hydrolysis was equal to the time constant describing the particle growth, demonstrating that this growth is limited by the hydrolysis.

In a subsequent paper Matsoukas and Gulari (9) developed a monomer addition model to describe the nucleation and growth of silica spheres in the presence of a rate-controlling hydrolysis of the monomers, which was characterized by the rate constant k_h. A particle is nucleated in this model if two monomers condense, a process described by the rate constant k_c. Growth takes place only through addition of hydrolyzed monomers (the concentration of which is represented by c_h) to the particle volume (V_p):

$$\frac{dV_p}{dt} \sim k_c \cdot R^\alpha \cdot c_h. \qquad [3]$$

Here, α describes the power-law dependence of the rate of incorporation of hydrolyzed monomers on the particle radius R. Different growth mechanisms are characterized by a different value of α; reaction- and diffusion-limited processes were looked at in detail.

In a reaction-limited process, the growth rate is limited by the condensation of hydrolyzed monomers on the particle surface. Thus, the rate of change in particle mass or volume is proportional to the particle surface and for smooth surfaces $\alpha = 2$. In a diffusion-limited process the growth rate is limited by the transport of monomers to the particle surface. If the diffusion of the monomer is much faster than that of the particles, the particle growth (Eq. [3]) is proportional to the radius of the particles and $\alpha = 1$. Different growth mechanisms for the incorporation of monomers do not influence the particle growth rate because the overall rate is limited by the rate of hydrolysis.

The polydispersity and final particle size, however, *are* affected by differences in the growth mechanism. The polydispersity is influenced, because particles of different size compete for monomers with efficiencies that depend on the growth mechanism (Eq. [3]). Thus, growth mechanisms for which the smaller spheres are growing faster than larger spheres are self-sharpening (see also Section II.B and (19)). The larger this difference in growth rate, the smaller a final polydispersity will become. It can be shown (10) that for diffusion-limited growth the relative standard deviation of the size distribution (σ) decreases with the mean radius of the spheres ($\langle R \rangle$) as

$$\sigma^2 \propto \langle R \rangle^{-3}. \qquad [4]$$

For reaction-limited growth the decrease in the polydispersity is less rapid:

$$\sigma^2 \propto \langle R \rangle^{-2}. \qquad [5]$$

By following the square of the relative standard deviation σ^2 of the size distribution as a function of the mean particle radius with TEM, Matsoukas and Gulari (9, 10) obtained an exponential of -1.75 ± 0.2, indicating a reaction-limited growth.

Within the assumptions made in the model by Matsoukas and Gulari it is very difficult to obtain expressions for the final particle size when $\alpha = 1$ or 2. Therefore, the diffusion- and reaction-limited processes are approximated

by $\alpha = 0$ and 3, respectively. For these values of α, relations can be derived between the rate constants k_c and k_h, the starting concentration of TES (c_0), and the (final) particle radius R:

$$R \sim \left(\frac{k_c}{k_h} \cdot c_0\right)^{1/9}, \quad \alpha = 0 \qquad [6]$$

$$R \sim \left(\frac{k_c}{k_h} \cdot c_0\right)^{1/6}, \quad \alpha = 3. \qquad [7]$$

As stated in the Introduction, Zukoski and co-workers model the particle formation and growth as an aggregation process of small subparticles or primary particles that are several nanometers in size. They based their model on observations made with TEM (11). Electron microscope grids were dipped into a solution in which the "Stöber" reaction took place and the particle size was followed as a function of time. It was observed that the particle volume grew exponentially in time, but that primary particles were visible until late in the reaction (see, however, the results of Bailey and co-workers described below). In their earlier papers (e.g., Ref. 11) it was stated that all TES was hydrolyzed in the first few minutes. This was based on ^{29}Si NMR. The primary particle nucleation was described using the classical homogeneous nucleation theory of a supersaturated solution and the nucleation was assumed to take place during the whole growth.

In order to derive quantitative results for the growth rate and polydispersity, theoretical coagulation calculations were made (12). In the mathematical model developed, the effects of the particle charge were incorporated via a numerical solution of the linearized Poisson–Boltzmann equation for two unequal spheres, dispersion forces were modeled using the microscopic theory of Hamaker, and diffusion coefficients were calculated on a two-particle level taking hydrodynamics into account. This controlled aggregation model, in which particles aggregate until the charge on the particles gets large enough to prevent aggregation between the larger particles, was based on a successful model to describe the formation of latex spheres. One of the most interesting conclusions made in (12) relating to the work described in our paper is that during the aggregative growth the exponent α in Eq. [3] never exceeds 1.7. Under most conditions and times investigated, it was closer to 1 than to 1.7 (12).

In subsequent papers (13, 14) kinetic measurements were fitted to the model presented in (12). Again by using ^{29}Si NMR the concentration of TES was followed as a function of time. The amount of soluble silica, i.e., silica not removed from the suspension by filtration, measured with atomic absorption was also followed. This time—contrary to what was reported in (11)—it was found that the decrease in both TES and soluble silica followed an exponential decrease in concentration with the same rate constant as described the increase in particle volume as a function of time. (These findings are in accordance with the results of Matsoukas and Gulari.) From these results it was not concluded, however, that the growth was rate-limited by the hydrolysis of the monomer, but instead that the polymerization was rate-limiting. It was argued that the observed equality of the rate constants could be explained by assuming a steady state concentration of TES that resulted from reversibility of the hydrolysis reactions.

Under influence of the results of Bailey and co-workers (see below), the formation of primary particles was not described anymore as a homogeneous precipitation, but as the formation of polymer structures that collapsed at a certain critical size to small primary particles. Most kinetic measurements reported in (13) were not performed by NMR or TEM, but by following the dispersion conductivity and volume.

In (14) it was shown that it was not possible to fit the experimental results with the aggregative growth model as proposed in (12). Besides the electrostatic repulsion and Van der Waals attractions, it was necessary to take a solvation force into account as well. Further-

more, it was assumed that the surface potentials of the particles of different size and suspended in different reaction mixtures were constant (−13 mV). This assumption was based on the observation that particles with radii from 25 to 350 nm suspended in ethanol containing 3.8–1.5 M H_2O and 0.5–3 M NH_3 all had the same mobility (-1.1×10^{-8} m^2 V^{-1} s^{-1}). It is not clear, however, if or to what extent differences in viscosity, dielectric constant, and dissociation of ammonium hydroxide in the different solvent mixtures were taken into account in the calculation of the surface potential. Finally, in order to fit the experimental data, primary particles of 1.5 to 4 nm were used in the calculations.

Harris and co-workers investigated the kinetics of the Stöber process using several experimental techniques (6, 7). The production of ethanol was followed with gas chromatography, the change in TES concentration was followed with Raman spectroscopy, and soluble silica (i.e., unreacted TES and monomer and some dimeric silicic acid) was analyzed by a color reaction (the molybdate method). Particle sizes and concentrations were followed with turbidity and dynamic light scattering measurements. The experimental data were analyzed by assuming that the hydrolysis, Eq. [1], was irreversible and that the condensation reactions, Eq. [2], were reversible in order to account for the small equilibrium concentrations of soluble silica that remained in the supernatant after the growth of the spheres.

As before, it was found that the hydrolysis of TES could be described by a first-order process. The dependence of the rate constant of hydrolysis and condensation on the concentration of NH_3 and H_2O and on the alcohol used was determined. As was expected for a nucleophilic base-catalyzed reaction mechanism (see, e.g., (17) for details on this mechanism), it was found that both hydrolysis and condensation were increased in a similar manner by an increase in the concentration of NH_3 and H_2O. The dependence of both reaction rates on the length of the cosolvent alcohol was the same as well. Experimentally, the following (irregular) order in the reaction rates was obtained: 1-butanol > methanol > 1-propanol > ethanol > 2-propanol.

In ethanol the kinetics were followed for two different concentrations of TES, but otherwise with the same conditions. The rate constant for the condensation (and dissolution) were the same in both cases *only* if the rate law of incorporation of hydrolyzed monomers and the dissolution of silica were chosen proportional to the particle surface. (The dissolution rate constant was found to be 500 times smaller than k_c.) It was therefore concluded in (7) that the particles grew primarily through the addition of monomers rather than through aggregation with primary particles.

Philipse measured the growth rate of a seeded suspension with time-resolved static light scattering (4). In modeling the obtained growth curves, i.e., particle radius versus time, the author assumed that the growth was limited by diffusion of subparticles (with radius of about 5 nm) against an unscreened coulomb potential (surface potential approximately 150 mV) of the growing spheres. One of the suggestions for further work was to verify the predicted strong increase in the particle growth rate if the ionic strength of the reaction mixture was increased.

Bailey and co-workers (15, 16) used cryogenic transmission electron microscopy in order to follow the particle formation and growth by direct observation of structures in the liquid state. The cryo-TEM technique makes this possible by cooling a holey carbon grid with thin liquid films of reaction medium so fast that the solvent mixture (propanol, water, and ammonia) vitrifies. The structures in the fast-frozen liquid films were imaged and the process of formation and growth of the particles was investigated. To prevent rupture of the films only the early reaction stages when the particles were small could be observed with the cryo-TEM method (16).

In the beginning of the reaction, low-density particles with an average size of 26 nm were

observed. Later on, high-density particles with a rough texture and an average size of 20 nm were seen next to some low-density structures. If the solution was dried on an ordinary TEM grid at that time in the reaction, high-density particles with an average size of 30 nm were seen together with many smaller particles also of high density. Some of the smaller particles appeared attached to the larger spheres, as opposed to the cryo-micrograph where no aggregation was observed. At longer times, only larger high-density particles and no low-density structure were imaged in the cryo-micrographs.

Bailey and co-workers argued that the small particles that were reported by Zukoski and co-workers (11) were artifacts caused by drying the reaction medium on the grid. Probably the ethanol evaporates faster than water and TES. In the remaining highly concentrated solution of TES in water, particles could be formed on the grid before complete drying. This would explain the finding of small particles (on the grid) during an important part of the growth. Furthermore, no dense particles in the size range 2–12 nm were seen in solution during the whole part of the reaction in which it was possible to follow the events with the cryo-TEM technique. Thus, no subparticles in the size range predicted by Zukoski and co-workers in their aggregation model (14) were seen. Therefore, it was proposed by Bailey and co-workers that particles grow during most of the time by addition of monomers and/or (small) polymer-like oligomers.

By using ^{29}Si NMR to follow the concentration of TES over time, it was found that besides the TES resonance only the peak of $Si(OCH_2CH_3)_3OH$ and no higher polymerized species could be observed during the entire reaction (16). The hydrolysis of the first ethoxy group could be described by a first-order process. Hydrolysis of the second group was faster than that of the first groups, roughly by a factor of 2. The experimental results seemed to indicate, however, that the species $Si(OCH_2CH_3)_3OH$ was not only participating in hydrolysis reactions as was assumed when the rate laws were integrated, but was also taking part in condensation reactions.

B. Competitive Growth in a Binary Mixture of Particles

By analyzing the competition for "building units" (monomers or other species that can condense on the particle surface) between two groups of particles of different size, the mechanism of incorporation can be analyzed. It does not make any difference if hydrolysis is the rate-limiting step in the growth or not, because at every instant in time, the different particles compete for the same concentration of condensable species. The measurement of the mean sizes in a bimodal distribution as proposed by Bradford *et al.* (18) for latex dispersions is of course easier and can be done more accurately than the determination of the standard deviation (or second moment) of *one* size distribution. Furthermore, it has been shown by Matsoukas and Gulari (10) that for certain values of α (Eq. [3]) it is not even possible to determine the growth exponent from the polydispersity.

First, it is assumed by Bradford *et al.* that the growth of spheres with particle volume V_p (or with radius R) can be described by an equation such as Eq. [3]:

$$\frac{dV_p}{dt} = R^{\alpha} \cdot f(c_h, [H_2O], [NH_3], t \cdots) \quad [8]$$

or

$$\frac{dR}{Rdt} = \frac{1}{4\pi} \cdot R^{\alpha-3} \times f(c_h, [H_2O], [NH_3], t \cdots). \quad [9]$$

Here, $f(c, [H_2O], [NH_3], t \cdots)$ is a function that is assumed to be the same for all particles and describes the dependence of the growth rate on all variables except the radius R of the particles. Thus, f depends on the concentration of the catalyst, the concentration of water,

and even on time, e.g., through the changing concentration of hydrolyzed monomers c_h.

Integration of Eq. [9] leads to

$$R^{3-\alpha} - R_0^{3-\alpha} = \frac{(3-\alpha)}{4\pi}\int_0^t f(t')dt'. \quad [10]$$

If we consider a bimodal distribution of particles with radii R_{0a} and R_{0b} ($R_{0a} > R_{0b}$) that has grown larger by addition of TES to radii R_a and R_b, then

$$R_a^{3-\alpha} - R_{0a}^{3-\alpha} = R_b^{3-\alpha} - R_{0b}^{3-\alpha} = \frac{(3-\alpha)}{4\pi}\int_0^t f(t')dt' \quad [11]$$

and after solving for R_a/R_b,

$$\frac{R_a}{R_b} = \frac{1}{\gamma}\cdot[\gamma^{3-\alpha} + \beta^{3-\alpha} - 1]^{1/(3-\alpha)}, \quad [12]$$

where $\beta = R_{0a}/R_{0b}$ and $\gamma = R_b/R_{0b}$.

From inspection of Eq. [9] or [12] it follows that if $\alpha < 3$ the *relative* distance in size decreases if the particles grow and therefore growth is self-sharpening. The convergence of the two sizes is faster for smaller values of the growth exponent α. If $\alpha = 2$ it follows from Eq. [9] that all particles increase their radius by the same amount. Thus, the absolute differences in particle radii stay the same and also the form of the size distribution does not alter in time. For $\alpha = 3$ the relative rate of growth in radius is independent of size and for $\alpha > 3$ a distribution that grows, becomes more polydisperse as the size increases.

C. *Particle Growth Measured by Static Light Scattering*

In the measurements reported in this paper the size of the particles and the refractive index difference with the solvent were always small enough for the Rayleigh–Gans–Debye (RGD) approximation to apply (20). In this approximation, the scattering particles interact only weakly with the incident electric field. For dilute dispersions interparticle interference is noncorrelated and the time-averaged intensity I is the sum of the scattered intensities of the separate particles.

In the following we consider a dilute suspension of homogeneous, spherical particles with radius R and number density C_n. For light polarized vertically to the scattering plane, the scattered intensity is given in arbitrary units by

$$I(KR) = C_n R^6 P(KR), \quad [13]$$

in which the length of the scattering vector K describes the dependence of the intensity on the scattering angle θ:

$$K = \frac{4\pi n_s}{\lambda_0}\sin(\theta/2). \quad [14]$$

Here, n_s is the refractive index of the suspension and λ_0 the wavelength of the incident light in vacuum.

The form factor $P(KR)$ describes the intraparticle interference. For all the measurements reported in this paper the intraparticle interference can be approximated further in the so-called Guinier region by (20)

$$P(KR) = \exp(-K^2R^2/5). \quad [15]$$

The assumption that the growing spheres are homogeneous has been confirmed by measurements on the properties of particles formed in different concentrations of ammonia and water (17) and by seeded growth experiments (4, 21, 3). Therefore, Eqs. [13] and [15] can be used to evaluate the mean radius as a function of time through the angle dependence of the scattered intensity. The "absolute" intensity provides information on the total scattering volume (Eq. [13]). By comparing the change in intensity with the change in particle radius it can be determined whether or when the number of particles C_n becomes/stays constant.

The strong particle radius dependence of the scattered intensity as given in Eq. [13] makes it difficult to obtain accurate data during the whole growth process, if the starting and final particle radii are not close together. Further-

more, Eqs. [13] and [15] are valid in the limit that the scattering is only caused by single scattering events (see, e.g., Ref. (22) for criteria to detect multiple scattering). The consequence is that if a dispersion of particles is grown from a radius of 20 to 80 nm and the final dispersion is not yet in the multiple scattering regime, the early particle growth cannot be followed. The reason is that the scattered intensity of the starting dispersion would be a factor $4^6 \simeq 4100$ times lower.

III. MATERIALS AND METHODS

A. Materials and Silica Dispersions

Ethanol (Merck), *n*-propanol (Baker), and $LiNO_3$ (Merck) were of analytical reagent quality. Ethanol and tetraethoxysilane (TES, Fluka, purum grade) were freshly distilled before each synthesis. Ammonium hydroxide (Merck, 25%, subsequently referred to as "ammonia") was of analytical reagent quality; one batch contained 14.0 mol/liter NH_3 and another contained 15.1 mol/liter NH_3 as determined by titration.

The synthesis of the seed and other silica particles (Table I) was done as described in the literature (see, e.g., Ref. (17)). All the concentrations of water and ammonia mentioned in this paper were calculated assuming all the added liquid volumes were additive. Weights of substances were converted to volumes by density data given in (23). Mixtures of ethanol and water show some volume contraction upon mixing; the calculated concentrations may, therefore, be used only for comparison with other data in mol/dm^3 given in the literature, and which were calculated using the same procedure.

TABLE I

Radii According to Transmission Electron Microscopy and Static Light Scattering

System	TEM (σ) (nm)	SLS (nm)
A6	89.4 (6%)	107.2 ± 0.3
A7[a]	93.2 (8%)	109.4 ± 0.4
A8[a]	154.3 (8%)	179.3 ± 0.4
A11	17.5 (18%)	20 ± 1
A12	45.1 (9%)	51.2 ± 0.5
A13	59.2 (8%)	73.5 ± 0.2
A14	142.0 (4%)	154 ± 1
A15	81.2 (5%)	91.6 ± 0.4
SG1	64.1 (6%)	73.3 ± 0.2
SG2	61.2 (6%)	70.1 ± 0.2
SG3	Fig. 2c	
SG4	65.2 (7%)	75.2 ± 0.1

[a] $[LiNO_3]$ = 1.0 m*M*; for A8 the salt was added before TES, and for A7 15 min after TES.

The volume fractions of silica that were used in the different experiments were calculated assuming a density of the particles of 2 g/ml. Weight fractions were determined by drying under a stream of dry nitrogen for 24 hours at 100°C.

The volume fractions ϕ of the silica particles used in the stability measurements are given in Table II. The following stability criterion was used: If no rapid flocculation of the particles was observed after addition of $LiNO_3$, the sedimentation rate was measured. After sedimentation to the bottom of the container, we tried to redisperse the particles by shaking. If this was successful and no flocs were seen in the dispersion, the sedimentation rate was measured again. A dispersion was termed stable if no change in the rate was observed. The range of concentration in $LiNO_3$ within, which the dispersion became unstable is given in Table II. Always at least two dispersions below and above the range given in the table were examined as well.

The particle volume fractions used in the competitive growth experiments are given in the legend to Fig. 1.

In the seeded growth experiments the volume fraction of the particles A11 was about 2×10^{-6} and that of A12 was around 3×10^{-5} (see Table III). The amount of TES, V_{TES2}, that had to be added to increase the radius from R_1 to R_2 is given by

$$V_{TES2} = V_{TES1}((R_2/R_1)^3 - 1). \quad [16]$$

Here, V_{TES1} is the volume of TES needed to

TABLE II

Particle Stability of Alcosols Probed by Addition of $LiNO_3$

Particles (radius)	ϕ^a (10^{-3})	$[NH_3]$ (M)	$[H_2O]$ (M)	$[LiNO_3]^b$ (mM)
A6 (108 nm)	1.0	1.1	3.0	3.9–4.5
A6 (108 nm)	0.67	1.1	3.0	3.9–4.5
A6 (108 nm)	0.5	1.1	3.0	3.9–4.5
A6 (108 nm)	1.0	0.81	2.1	5.7–6.4
A6 (108 nm)	1.0	3.3	9.0	3.9–4.5
A6 (108 nm)	1.0	1.1	9.0	5.1–5.7
A13 (74 nm)	1.0	0.81	2.1	5.1–5.7

[a] Particle volume fraction.

[b] Limit concentrations bounding the concentration of $LiNO_3$ at which stability was lost.

prepare the particles with radius R_1. In the derivation of this formula it is assumed that all the added TES grows on the existing particles and that the density of the added layer is the same as that of the core on which it grows. It has been shown elsewhere that these assumptions are correct (3, 4, 17, 21).

B. Electron Microscopy

Transmission electron micrographs were made by dipping copper 400-mesh carrier grids in a dilute dispersion. The grids were covered with carbon-coated Formvar films and the photographs were made of particles retained on the film. A Philips CM10 transmission electron microscope was used, with the magnification calibrated with a diffraction grating.

Particle radii of several hundred particles were measured using an interactive image analysis system (IBAS). Assuming a spherical shape, the surface of the particles was used to determine a number-averaged particle radius $\langle R \rangle$ and the relative standard deviation σ as defined by (see Table I)

$$\sigma^2 = \frac{\langle R^2 \rangle - \langle R \rangle^2}{\langle R \rangle^2}. \qquad [17]$$

For the competitive growth experiments use was also made of a dispersion of "calibration" particles with a very small polydispersity (R = 450 nm, σ = 1.6%, Fig. 2a). These calibration particles were added because it was found that the absolute particle sizes were not perfectly reproducible. These unknown errors could be eliminated by using the large spheres as an internal standard.

C. Light Scattering

Light scattering measurements were made at 20.0 ± 0.1 and 25.0 ± 0.1°C. Dispersions were made dust free by filtering through Millipore filters (pore diameter typically five times the particle diameter). Cuvets with a diameter of 2 cm were cleaned by continuous rinsing with freshly distilled acetone.

The "not-time-resolved" static light scattering measurements were made with a Fica-50 photometer using vertically polarized incident and detected light (λ = 436 and 546 nm). A correction was made for scattering of the solvent. Mean intensities as a function of

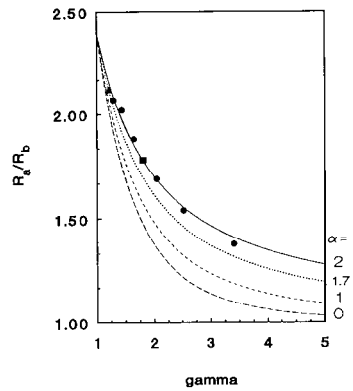

FIG. 1. Competitive growth of a bimodal dispersion (A13 and A14) with initial size ratio β = 2.40. The final size ratio R_a/R_b is plotted against the relative increase in radius of the smallest spheres $\gamma = R_b/R_{ob}$. (●) Total particle volume fraction approximately 5×10^{-5}, number density of A13 and A14 approximately equal, $[NH_3]$ = 1.0 M and $[H_2O]$ = 2.4 M; (■) total particle volume fraction approximately 1×10^{-4}, everything else the same as with ●; (▲) $[NH_3]$ = 0.45 M and $[H_2O]$ = 1.05 M, everything else the same as with ●, a second nucleation was observed.

TABLE III

Kinetic Measurements with ^{13}C Nuclear Magnetic Resonance (NMR) and Static Light Scattering (SLS): Rate Constant k, Induction Time t_1, and Scattering Volume Exponent ω

Particles (solvent)	$[NH_3]$ (M)	$[H_2O]$ (M)	k ($10^{-3} \cdot min^{-1}$)	t_1 (min)	ω	Method
A11	1.20	2.98	10.8 ± 0.3	44 ± 1	6.03 ± 0.08	$y = \{I(K=0)\}^{1/2}$
Ethanol						SLS; [TES] = 1.6 mM
A11	1.20	2.98	11.4 ± 0.3	45 ± 1		$y = R^3$
SG1	1.32	3.27	16.1 ± 0.2	19.7 ± 0.8	6.41 ± 0.07	$y = \{I(K=0)\}^{1/2}$
Ethanol						SLS; seeded growth
SG1	1.32	3.27	16.1 ± 0.2	18.3 ± 0.9		Seed: A11
						$y = R^3$
SG2	1.30	3.22	15.7 ± 0.3	18 ± 1	6.3 ± 0.1	$y = \{I(K=0)\}^{1/2}$
Ethanol						SLS; seeded growth
SG2	1.30	3.22	15.9 ± 0.3	19 ± 1		$[LiNO_3]$ = 1.0 mM;
						Seed: A11
						$y = R^3$
SG3	1.95	4.58	36.1 ± 0.6	11 ± 1	9.4 ± 0.2	$y = \{I(K=0)\}^{1/2}$
Ethanol						SLS; seeded growth
SG3	1.95	4.58	42.4 ± 0.7	7 ± 1		Seed: A11
						$y = R^3$
SG4	0.660	1.77	6.21 ± 0.08	15 ± 1	6.4 ± 0.1	$y = \{I(K=0)\}^{1/2}$
Propanol[a]						SLS; seeded growth
SG4	0.660	1.77	6.15 ± 0.08	17 ± 1		Seed: A12
						$y = R^2$
P2	0.668	1.80	6.1 ± 0.2	0	—	Ethoxy decrease
Propanol[a]						NMR; [TES] = 0.167 M
P2	0.668	1.80	5.9 ± 0.2	0	—	Ethanol increase

[a] 25.0°C; others at 20.0°C.

the scattering angle were obtained in the range $20° \leq \theta \leq 150°$ (see Table I).

Time-resolved static light scattering measurements were made with an apparatus that will be described in more detail elsewhere (see (24); parts of the setup are also described in (25)). The scattered light of a dispersion is focused by means of a circular thermostating bath on 140 optical fibers that are placed around the cuvet in a semicircle. The 140 bundled fibers are imaged on a one-dimensional diode camera containing 512 pixels (EG&G, model 1452A). The diode camera has a dynamic range of 2^{14} and a time resolution of 10 ms. The measured intensities are processed with a microcomputer. A He/Ne laser (Spectra Physics 125A) is used as a light source. It is clear that this setup, in which the whole scattering curve is obtained at once during a very short measuring time, is very well suited to follow the dynamics of the growth of scattering spheres.

The scattering curves of the growing particles were analyzed after calibration and correction for solvent scattering in the K-range $KR < 1.5$ with Eq. [15].

D. *Hydrolysis Followed by ^{13}C NMR*

High-resolution ^{13}C NMR measurements of TES in solution were made on a Bruker AM 500 spectrometer. The ^{13}C 90° pulse length

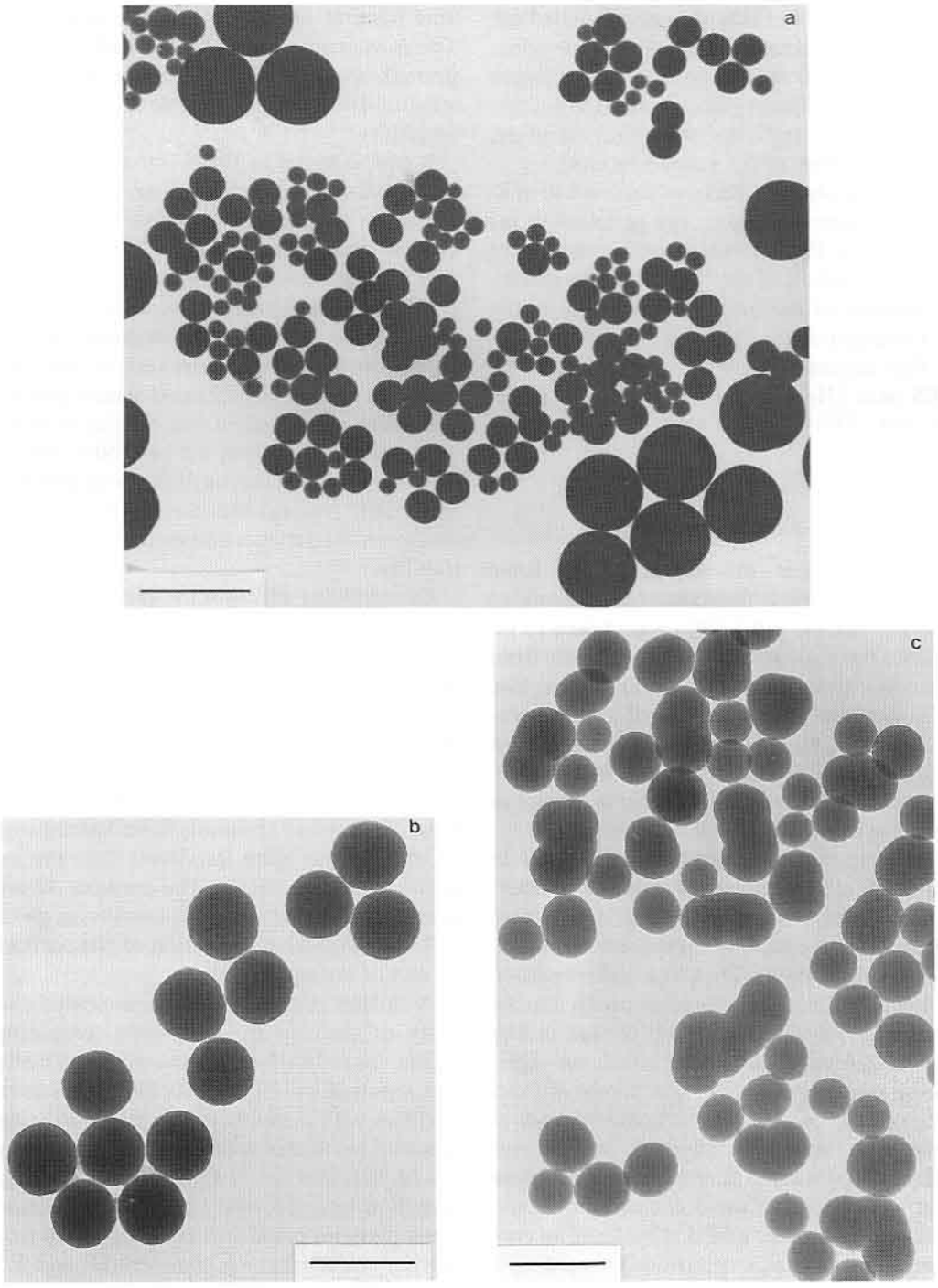

FIG. 2. Transmission electron micrographs. (a) Example of the competitive growth of A13 and A14 together with larger calibration particles (bar 1 μm). (b) Particles A15, the growth of which was followed with static light scattering (bar 250 nm). (c) Seeded growth of A11 at excessive concentrations of ammonia and water (SG3) (bar 250 nm).

was 5 μs and 240 FIDs were accumulated per spectrum. To decrease the spin–lattice relaxation times, 10 mg of the relaxation reagent chromium(III)acetylacetonate ($Cr(acac)_3$) was added per milliliter of solvent; therefore, repetition times of 0.5 s could be used.

The hydrolysis of TES was followed in mixtures of ammonia, water, and propanol by integration of the decreasing peak intensity of the C–O carbon of the ethoxy group and by integration of the increasing intensity of the C–O carbon of the liberated ethanol.

The concentrations for the hydrolysis of TES were $[H_2O] = 1.80\ M$, $[NH_3] = 0.668\ M$, and $[TES] = 0.167\ M$.

IV. RESULTS AND DISCUSSION

A. Additions of $LiNO_3$

To investigate the effects of the ionic strength on particle formation (or nucleation) and growth, the salt $LiNO_3$ was chosen to influence the ionic strength independently from the concentrations of NH_3 and H_2O that also influence the concentrations of ions in solution. $LiNO_3$ was chosen because it is known to dissociate 94% at $10^{-2}\ M$ and 99% at $10^{-3}\ M$ in pure ethanol (26). If water is present as well, the dissociation will be even higher.

At first the concentrations of $LiNO_3$ at which an alcosol remained stable were determined. A dispersion was termed "stable" (see Materials and Methods), if the sedimentation rate was unaltered after a first sedimentation to the bottom of the container under gravity. This criterion of stability was chosen to find the concentration of salt at which no aggregation occurred over a longer period of time. Then, these concentrations could be used to determine levels of addition to growing spheres. For such a purpose a concentration that would mark a rapid coagulation in seconds would be less useful. The limiting concentrations of $LiNO_3$ determined according to the above-mentioned stability criterion are given in Table II.

The point at which the instability was detected was not shifted by a change in the volume fraction of the particles A6 (Table II). This is what one would expect if only the ionic strength of the dispersion and not specific adsorption effect was responsible for the particle instability.

It can be found in Table II that an increase in the water concentration from 3.0 to 9.0 M caused an increase in the particle stability. An increase in the concentration of NH_3 from 1.0 to 3.3 M, however, resulted in a decrease in stability. This last result is not what one at first hand would expect. The negative surface charge on the silica spheres results from dissociation of the (slightly) acid silanol groups. Therefore, it is expected that both an increase in the concentration of the base NH_3 and an increase in $[H_2O]$ (through the production of more OH^-) would increase the net negative charge on the particles and thereby the particle stability.

Destabilizing effects of the addition of NH_3 may result from an increase in the ionic strength through the production of ions (the increase in the dielectric constant of the medium is probably small). The ions decrease the double layer thickness and lead to a dispersion that is more easily flocculated (see, e.g., (27)). Apparently, at certain concentrations of water and ammonia these destabilizing effects become more important than the increase in surface charge. The particles A6 are even the most stable (of the conditions given in Table II) at a concentration of NH_3 of 0.81 M and of H_2O of 2.1 M.

A further indication of the decreased stability of particles in dispersions containing higher concentrations of ammonia and water was reported in (28). It was found that even particles with a radius of 200 nm slowly aggregated in ethanol containing approximately 2.5 M NH_3 and 6.6 M H_2O. This was not aggregation in a secondary minimum, because these particles could not be repeptisized in a solvent containing, e.g., 0.6 M NH_3 and 1.7 M H_2O. The flocculation in the primary minimum was probably followed by a chemical reaction between the surface silanol groups. If the particles were, however, transferred im-

mediately after the synthesis to such a solution containing less ammonia and water, the sol remained stable for years.

It is, disappointingly, difficult to support the stability measurements with calculations because many essential parameters are unknown and difficult to obtain or estimate. For instance, the dissociation constants of the silanol groups and ammonium hydroxide in the reaction mixtures are unavailable and even solvent properties like dielectric constant and viscosity are unknown. The DLVO (Derjaguin, Landau, Verweij, and Overbeek) theory on the stability of charged particles (27) does predict that under otherwise identical conditions the stability decreases with the particle radius. This explains the (slight) decrease in stability of the particles A13 compared to A6 in the solvent mixture containing 0.81 M NH_3 and 2.1 M H_2O. It is clear, however, that the complex stability behavior of the silica particles in mixtures of ammonia, water, and ethanol warrants further research. To make quantitative predictions, the dependence of the surface potential and ionic strength on the concentrations of water and ammonia needs to be known.

Second, $LiNO_3$ was added prior to and during the particle formation and growth. The results of these additions to the final particle size of silica spheres prepared in a mixture containing 2.65 M H_2O and 0.986 M NH_3 are given in Table I. With a concentration of $LiNO_3$ of 1 mM the final dispersions were stable and unclustered as indicated by light scattering; at 2 mM the particles flocculated during the growth and consisted of irregular, nonspherical structures (see, e.g., Fig. 2c). Addition of the salt before TES was added resulted in a significant increase in size from 107 to 179 nm, while addition after the first turbidity appeared (15 min) had hardly any effect on the final particle size.

The influence of the ionic strength on the final particle size and the stability measurements of A6 and A13 are clearly related and provide information on the mechanism of particle formation. These subjects are discussed further in the section on the mechanism of formation and growth, after the effects of $LiNO_3$ addition on the rate constant of the particle growth have been discussed.

B. Competitive Growth

Suspensions containing particles of two mean sizes (A14 $\equiv R_{0a}$ and A13 $\equiv R_{0b}$, see Table I) with a size ratio $\beta = 2.40$ were grown larger by addition of TES. In Fig. 1 the resulting size ratio is plotted as a function of the ratio γ of the smallest spheres after and before the growth step. An example of a typical electron micrograph (after growth) is given in Fig. 2a. A nonlinear fit of the experimental points to the competitive growth Eq. [12] resulted in a growth exponential $\alpha = 2.02 \pm 0.04$, indicating reaction-limited growth. The finding of a reaction-limited growth mechanism confirms the growth mechanism reported by Matsoukas and Gulari (8–10); however, they based their conclusion on much less accurate measurements of the polydispersity (or second moment) of a single size distribution.

Besides the theoretical line of reaction-limited growth in Fig. 1, curves for diffusion-limited growth ($\alpha = 1$), growth independent of the particle size ($\alpha = 0$), and the maximum growth exponent predicted by Kim and Zukoski (12) in their aggregative growth model are drawn ($\alpha = 1.7$).

As explained in Section II.B, the growth exponent determines how the polydispersity decreases with increasing mean particle size. For $\alpha = 2$ all particles in the distribution increase their radius by the same amount, meaning that the absolute size differences stay the same and σ is simply proportional to $1/R$.

C. Kinetics

Hydrolysis followed with ^{13}C NMR. The hydrolysis of TES was followed with solution ^{13}C NMR, because then both the unhydrolyzed ethoxy groups and the produced ethanol molecules can be followed in time. For this to be possible, n-propanol was chosen as the cosolvent for TES. The chemical shift difference

of the carbon bonded next to oxygen that either belongs to an ethoxy group or an ethanol molecule is small (28). However, in solution NMR the small linewidth makes this chemical shift difference more than sufficient to analyze both the unhydrolyzed (at 60.8 ppm) and the hydrolyzed (at 58.8 ppm) groups separately (see Fig. 3).

The integrated intensities of both NMR signals were analyzed by assuming first-order kinetics. The pseudo-first-order rate constants obtained from the disappearance of ethoxy peaks and the appearance of ethanol (see Fig. 3) are given in Table III. These rate constants are called pseudo, because they depend on the *reactant* water concentration. Water is available in excess and therefore first-order kinetics are observed (see Fig. 4) as has been reported in the literature (7, 8, 16). Of course, the representation of the four hydrolysis steps (Eq. [1]) by only one rate constant is an approximation. As a first approximation, it is justified by the results (see also the data in (7, 8, 16) and the limited accuracy of the NMR method. As it should be, the rate constants obtained from both the loss of ethoxy and the production of ethanol are equal, given the experimental uncertainties (Table III). During the entire reaction there were no peaks visible that could be assigned to propoxy groups bonded to silicon. This means that, under the conditions of this study, reesterification of hydrolyzed TES or the exchange of an ethoxy group for an propoxy group is unimportant for soluble silicon species, contrary to the proposal made by Zukoski and co-workers in (13).

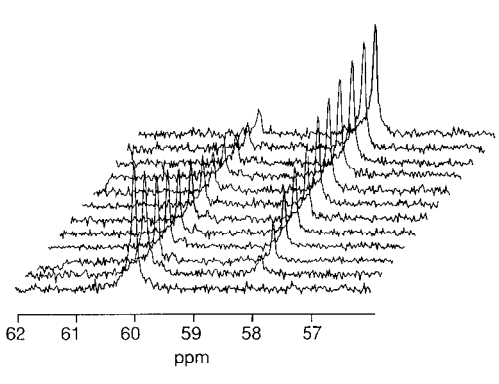

FIG. 3. ^{13}C NMR peaks of the carbon bonded to oxygen and belonging either to an ethoxy group of a TES molecule (60.8 ppm) or to a hydrolyzed ethanol molecule (58.8 ppm) as a function of time. The time difference between the curves is 28.8 min, [TES] = 0.167 M, [NH_3] = 0.668 M, and [H_2O] = 1.80 M.

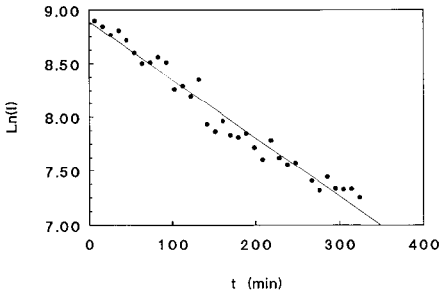

FIG. 4. Logarithm of the integrated intensity of the ethoxy carbon NMR signal versus time (experimental conditions given in the legend to Fig. 3).

Particle growth followed with static light scattering. As was explained in the theoretical section (II.C), the final volume fraction of particles with a radius between 50 and 100 nm has to be small to avoid the problem of multiple scattering. Therefore, if no seeded growth technique is used, the concentration of TES has to be much lower than the usual value of ~0.17 M (2, 3). (A synthesis with 0.17 M TES results in a particle volume fraction around 5×10^{-4}.) After many trials it was found that at a concentration of 1.20 M NH_3, 2.98 M H_2O, and 1.6 mM TES a monodisperse dispersion, A15, could be prepared (see Fig. 2b and Table I). The volume fraction was low enough to neglect multiple scattering. Some of the scattering curves as a function of time are given in Fig. 5. The points were plotted as $\ln(I)$ versus K^2, a so-called Guinier plot, because of the relation given in Eq. [15]. The growth of the spheres was analyzed by the change in particle radius R versus time and by the change in the scattered intensity at zero scattering angle versus time. The part of the scattering curve where Eq. [15] was valid provided the sphere radius through the angle dependence of the scattering; this relation was also used to extrapolate the experimental in-

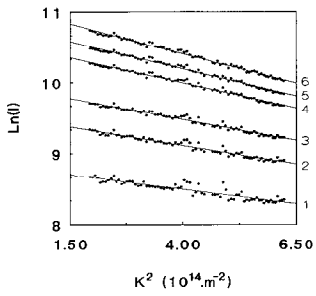

FIG. 5. Guinier plots, logarithm of the scattered intensity versus the square of the scattering vector K, of the growth of A15 versus time. Curve 1, 80 min; 2, 100 min; 3, 120 min; 4, 140 min; 5, 180 min; and 6, 18 h.

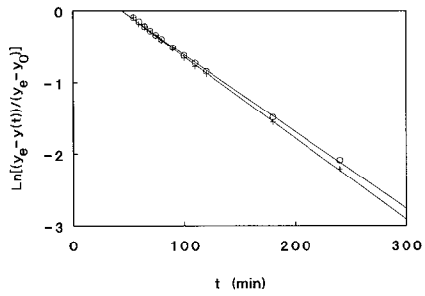

FIG. 6. Growth of A15 followed with static light scattering; (○) $y = \{I(K = 0)\}^{1/2}$, (+) $y = R^3$.

tensities to $K = 0$. It has been shown in the literature (17) that during the growth the scattering properties of the condensed material do not alter. Therefore, there is a linear relation between the amount of scattering particle volume and the number of moles of TES used to form this amount of silica. If we now assume that the number of growing particles is constant and that the growth is limited by the first-order hydrolysis rate of TES, then the growth of the particle volume can be described by a first-order process as well:

$$\ln\left(\frac{y_e - y(t)}{y_e - y_0}\right) = -k \cdot t. \qquad [18]$$

Here y is proportional to the particle volume. Thus, $y \propto R^3$, with R obtained from the slope of a plot of $\ln(I)$ versus K^2 (Eq. [15]), or $y \propto [I(K)]^{1/2}$ (Eq. [13]). y_e stands for the final particle volume and y_0 stands for the starting volume in seeded growth experiments.

The results of the analysis of the growth data of A15 with Eq. [18] are given in Fig. 6. The curves are perfectly linear and the rate constants obtained are equal given the experimental uncertainties (Table III). Apart from an induction time, which is not predicted by Eq. [18], the underlying assumptions in deriving this equation seem to be correct. The probable reason for the induction period will be discussed below, when the seeded growth experiments are discussed.

As another check for the consistency of the experimental data and to determine the point where the number of particles was no longer constant, the logarithm of the intensity at $K = 0$ was plotted against the logarithm of the radius. As suggested by Eq. [13] the slope should be 6. The experimental slope determined from the linear plot (Fig. 7) was 6.03 (Table III). There is no deviation from the fitted line in Fig. 7. This indicates that the number of particles is constant from the first point that was analyzed (for this point the radius was already 49 nm).

With ammonia and water concentrations somewhat different from that used in the synthesis of A15 it was not possible to obtain a monodisperse suspension at low enough volume fraction. Therefore, it was decided to use a seeded growth technique (4) starting with the small particles A11 (Table I). Again a perfect fit to Eq. [18] was found (see Fig. 8) and the $\ln(I)$ versus $\ln(R)$ plot is linear as well (SG1, Fig. 9 and Table III). The obtained ex-

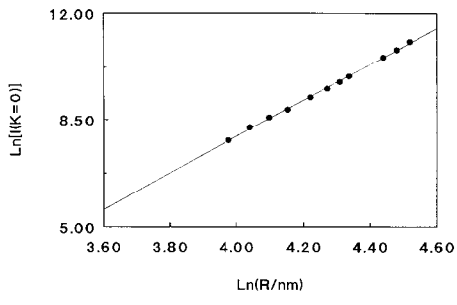

FIG. 7. Dependence of the forward scattered intensity on the particle radius of A15.

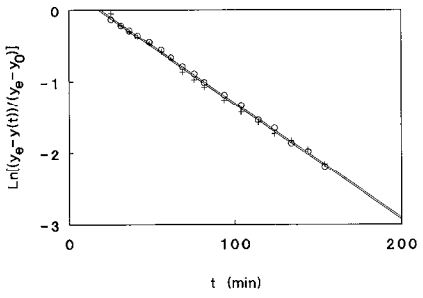

FIG. 8. Seeded growth of SG1 followed with static light scattering; (○) $y = \{I(K = 0)\}^{1/2}$, (+) $y = R^3$.

ponent from Fig. 9, 6.41, seems to be too high. However, Eq. [18] is correct for a monodisperse suspension of spheres and the starting seed suspension A11, Table I, is clearly polydisperse. If the polydispersity is taken into account (see, e.g., 21) it can be found that

$$I(K = 0) = \frac{\langle R^6 \rangle}{\langle R^3 \rangle} \qquad [19]$$

and

$$R_g^2 = \frac{\langle R^8 \rangle}{\langle R^6 \rangle}, \qquad [20]$$

where the brackets $\langle \ \rangle$ stand for number averaging and R_g stands for the optical radius obtained in the Guinier approximation with Eq. [15]. If we assume a starting Gaussian size distribution with a polydispersity of 18% and that this polydispersity decreases as $1/R$ (see Section IV.B) we can calculate the exponent by using Eqs. [19] and [20]. A value of 6.5 is obtained, which is not too far from the experimental result.

Under almost the same conditions the seeded growth experiment SG1 was repeated but now with an increased ionic strength by addition of $LiNO_3$ to a concentration of 1 mM, SG2. Both the rate constants and the induction time were identical (see Table III). This result is discussed further in Section V.

One result that is not explained by the assumptions made to derive Eq. [18] is the clear induction time (see, e.g., Fig. 8 and Table III) that is present in the growth curves. In a seeded growth experiment there is particle surface available from the moment TES is added and starts to hydrolyze (see also the section on the NMR results). However, just after the addition of TES one of the assumptions made cannot be true. No matter how much faster the condensation reaction is, there will always be a small period of time when the condensation rate is rate-determining, because the concentration of hydrolyzed TES builds up from a zero value.

To make an estimation of the role that the finite rate of condensation plays, the following simplified model was assumed. Besides a (pseudo) first-order hydrolysis process of TES, described by k_h, the condensation of a hydrolyzed monomer with the silica particle surface was also assumed to take place through a pseudo-first-order reaction in the concentration of hydrolyzed TES (described by k_c). Again this rate constant is "pseudo" because, apart from the justified assumption that the concentration of water is more or less constant, it is also assumed that the total surface of the silica particles is constant. (Certainly, the surface is changing in time and therefore k_c is a kind of mean rate constant as will be discussed below.) Under these assumptions the following, modified form of Eq. [18] can be derived:

$$\ln\left(\frac{y_e - y(t)}{y_e - y_0}\right) = \ln\left[\left(\frac{k_h}{k_c - k_h}\right) \cdot (\exp(-k_h t) - \exp(-k_c t)) + \exp(-k_h t)\right]. \qquad [21]$$

If $k_c \gg k_h$, the term $\exp(-k_c t)$ can be neglected

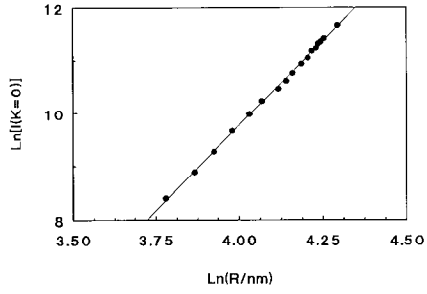

FIG. 9. Dependence of the forward scattered intensity on the particle radius of SG1.

at longer times and Eq. [21] can be approximated by

$$\ln\left(\frac{y_e - y(t)}{y_e - y_0}\right) = \ln\left(\frac{k_c}{k_c - k_h}\right) - k_h t. \quad [22]$$

We can now solve the long time result, which is linear in t, for the induction time t_I (the time at which the line defined by Eq. [22] goes through the time axis):

$$k_c = \frac{k_h \cdot \exp(k_h t_I)}{1 - \exp(k_h t_I)}. \quad [23]$$

If we now take the experimental values for the synthesis of SG1 (Table III), a condensation rate constant of 0.0611 min^{-1} is calculated. In Fig. 10 this value is used in a plot of the right-hand side of Eq. [21] versus time. The straight line represents the experimental data from Fig. 8 with slope -0.0161 min^{-1} and induction time 19 min. The calculated deviations from the straight line are small. Therefore, the induction time in the growth experiments is explained well by a finite rate of the condensation.

If a large particle is grown larger, e.g., from radius 350 to 353 nm, the surface area is approximately constant and the induction time would even provide an easy way to obtain accurate condensation rate constants through Eq. [23].

If one calculates the mean condensation rate constant for the growth of A15, one obtains $k_c = 0.0284$ min^{-1}. Although the growth rate is slower for the synthesis of A15 compared to that of SG1 (because of a lower water and ammonia concentration) the relative decrease in k_c is larger than that of the constant describing the growth. For A15 k_c is 2.6 times as fast as the constant that describes the growth and for SG1 3.8 times as fast. Probably, this difference is caused by the fact that for SG1 there already was a starting silica surface when TES was added; such a surface still had to be formed in the synthesis of A15. Therefore, in the synthesis of SG1 the pseudo condensation constant would seem larger because of the larger surface area available to hydrolyzed monomers in the induction time.

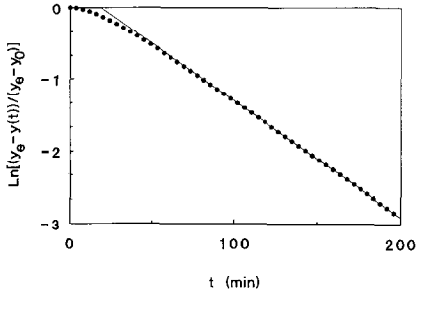

FIG. 10. Theoretical growth curve (●) using Eq. (20), $k_h = 0.0161$ min^{-1}, $k_c = 0.0611$ min^{-1}, and $t_I = 19$ min. Drawn line represents the experimental data of the growth of SG1 (Fig. 8).

The seeded growth experiment SG3 was performed in a higher concentration of ammonia and water (Table III). What happened during the growth is visible in the transmission electron micrograph in Fig. 2c: an important fraction of the seed particles aggregated during the growth. It should be stressed, however, that no signs of flocculation could be seen by visual observation during or after the growth. Further, after a few months the resulting dispersion SG3 was still stable. Nevertheless, it is clear from Fig. 2c that during the growth an aggregation of particles took place. As can be seen in the figure, the aggregates grew larger, after being formed early in the reaction, in a similar way as a large number of single particles. All the formed structures remained colloidal stable after the growth.

The aggregation during the growth was caused by two factors. First, at higher ammonia and water concentrations the particle stability decreases (see Section IV.A) and second, during the first part of the growth the ionic strength increases. This increase in ionic strength is related to the induction period. Both result from an initial increase in the concentration of hydrolyzed TES when the rate of hydrolysis is not yet rate-limiting. The dissociating silanol molecules cause the increase in the conductivity and ionic strength as has been reported in (13). As hydrolysis becomes rate-limiting and the TES concentration decreases, the pseudo-steady-state concentration

of hydrolyzed TES decreases and the aggregation stops. Again the importance of the ionic strength on the formation of the particles is demonstrated.

Although all the measured scattering curves were still quite linear (probably because the aggregation was not too severe) it can be seen in Table III that the rate constants and induction times obtained from the $y = R^3$ and $y = I(K = 0)^{1/2}$ plots are no longer the same. Further, the exponent describing the dependence of the scattering particle volume is too high. These inconsistencies show that the assumption that the number of particles is constant is invalidated. Still, it can be concluded that hydrolysis and condensation are strongly increased at these concentrations of ammonia and water.

Another important seeded growth experiment, now using the particles A13 as seeds, was performed in the same reaction mixture in propanol in which the NMR hydrolysis measurements were made, SG4. Within experimental error, the hydrolysis rate constant and the growth rate constant were equal (Table III), justifying the derivation of Eq. [18], and were in accordance with the results of Matsoukas and Gulari (8) and with the conclusion that hydrolysis is the rate-limiting step in the growth.

The seeded growth experiment SG4 was performed with the seed particles A12, because with the seed particles A11 almost the same "aggregation during growth" results were obtained as with the seeded growth of SG3. With A12 no irregularities were observed with TEM and the light scattering results were consistent as well.

V. PARTICLE FORMATION AND GROWTH MECHANISM AND SUMMARY

In this section we discuss the experimental results presented in this paper and in the literature in the light of a proposed particle formation and growth mechanism. Further, the mechanism is compared with those already presented in the literature (Section II.A).

First the overall rate of the particle growth is discussed. The growth of the particle volume was described by an exponential after an initial induction time, as was found by us with static light scattering and was reported by others as well (7, 8, 13). Despite the observations of Matsoukas and Gulari that the rate constant describing the particle growth equaled that of the first-order constant describing the hydrolysis of the monomers, it was not accepted by Zukoski and co-workers (13, 14) that the rate-determining step in the growth is the hydrolysis of the monomers. Instead, they proposed that the reversal of hydrolysis, reesterification, could be important as well and that the concentration of TES was actually a steady state concentration, while the rate-limiting step had to be found somewhere in the condensation pathway (13, 14). In order to eliminate this possibility, we used ^{13}C NMR to follow the hydrolysis of the ethoxy groups, the production of ethanol, *and* the eventual esterification of hydrolyzed TES with propanol. No esterification was found and the first-order rate constant of the disappearance of ethoxy groups equaled that of the production of ethanol. No induction time was observed. By following a seeded growth of particles in the same reaction mixture with static light scattering, the same rate constant was obtained. Therefore, it is concluded by us that during most of the growth process the production of hydrolyzed monomers is rate-limiting.

The presence of an induction time in a seeded growth experiment, where no particle nucleation is necessary, makes it clear that shortly after the addition of TES the rate of condensation is not yet high enough compared to the rate of production of hydrolyzed monomers. It was shown by using a simple model that a first-order condensation constant three times as large as the hydrolysis rate constant can still be the cause of a significant induction time. Under well-chosen conditions, the induction time can even provide a value for the condensation rate constant in a simple procedure.

Despite the fact that the rate of particle growth is limited by hydrolysis and therefore

no information about the condensation mechanism can be obtained from the growth rate, the desired information can be obtained by using a competitive growth procedure (18). At every instant in time there is a certain concentration of condensable species in solution. If there are particles of different size in the dispersion, the chance that a hydrolyzed species reacts with a particle of a certain size is determined by the (local) growth mechanism. Matsoukas and Gulari analyzed the polydispersity as a function of the mean particle size and found a reaction-limited process. By using a bimodal size distribution, we were able to determine the growth exponent α accurately and confirmed the finding of a surface reaction-limited growth. Although it is of course not possible to distinguish between a particle growth that is the result of addition of monomers, dimers, trimers, or small oligomers, it was possible to discriminate against a mechanism in which the growth results from the aggregation of subparticles a few nanometers in size (12). Indirect evidence against an aggregation process later in the particle growth was obtained by us with TEM (17) and was also concluded from the cryo-TEM results of Bailey *et al.* (16) (see Section II.A). Still further evidence against growth by aggregation is found in the fact that the growth rate is not influenced by changes in the ionic strength of the dispersion medium.

As far as the particle formation or particle nucleation is concerned, we do not agree with the kinetic model of Matsoukas and Gulari. The parameters that govern the final particle size in their model are given in Eqs. [6] and [7] (see Section II.A). It is well known that at an initial concentration of TES of 0.17 *M* particles can be synthesized with radii ranging from ~20 to ~400 nm (2, 3) by changing the concentrations of ammonia and water. This size range requires a change in the ratio of the condensation and hydrolysis rate constants of at least $20^6 = 64 \times 10^6$. Clearly, this is an erroneous prediction, even more so if one considers that the mechanisms of condensation and hydrolysis are similar (a nucleophilic SN2 mechanism) and that therefore both rates are influenced similarly by changing concentrations of water and ammonia (6, 7). Equations [6] and [7] also cannot explain why the hydrolysis rate is unaltered by addition of $LiNO_3$, while the final radius is significantly increased.

We agree with Zukoski and co-workers that the colloidal stability is an important factor in the mechanisms describing how many particles are formed early in the reaction and at what size these particles obtain the colloidal stability that prevents further aggregation. The fact that an aggregation process is occurring (but only early in the reaction) is demonstrated by the sensitivity of the final size on addition of $LiNO_3$ and by the observation that salt added after the induction period, at a point where aggregation is probably not important anymore, does not change the final size. Therefore, besides the concentration of ammonia and water, the ionic strength can also be used to influence the final particle size. The number of ions determines the particle size at which colloidal stability is reached and when the aggregation stops; a smaller number of growing particles results in a larger final particle size.

The explanation for the strong dependence of the final particle size on the concentration of ammonia and water is supported by the stability measurements performed with the same particles in different mixtures of ethanol, ammonia, and water. It was found that at low concentrations of NH_3 the particle stability is higher. This is also the limit in which small particles are formed (2, 3). Two effects make the stability behavior complicated. On the one hand an increase in the concentration of the base NH_3 and water will increase the surface charge through the dissociation of silanol groups and will thus stabilize the particles. On the other hand increasing the concentration of ammonia and/or water will increase the concentration of NH_4^+ and OH^- and thereby decrease the double layer thickness.

Another factor that is important for the particle stability during the aggregation process

early in the reaction is illustrated in the seeded growth experiment SG3 and the conductivity measurements of Zukoski and co-workers (13). Shortly after the addition of TES the conductivity increases until a pseudo-steady-state concentration of dissociating hydrolyzed TES is reached. During subsequent growth, the concentration of TES slowly decreases and the pseudo-steady-state concentration of hydrolyzed species follows until at the end of the growth the background reaction medium conductivity is reached. Therefore, the growing seed particles A11 aggregated during the growth in SG3, because they were already less stable in the relatively high ammonia concentration, and became unstable after the increase in the ionic strength after TES started to hydrolyze. After the growth, when the ionic strength dropped again, the final spheres and aggregates were stable again.

Thus, experiment SG3 mimics what happens during the early particle formation in a nonseeded particle synthesis. Depending on the ionic strength during the growth and on the surface potential on silica, small siloxane moieties (either polymer-like or condensed subparticles, see (16) aggregate until colloidal stability is achieved. If the particles are very stable (e.g., at low concentrations of ammonia) the aggregation stops relatively early and a larger number of particles grow to a small final size. Because in this case the silica layer that is deposited after the aggregation is thin, the resulting particles are not yet very spherical and the surface will be rough (see (17)). At high ammonia concentration the aggregation continues longer and only a relatively smaller number of particles becomes stable. This time, the amount of TES available per particle is larger, and a smooth almost perfect spherical particle with a polydispersity decreasing as $1/R$ is the result.

In conclusion, it can be stated that the general mechanism behind particle formation and growth is now clear. A lot has to be done, however, before the final particle size and polydispersity can be predicted without any adjustable parameter. In order to do this, the complex stability behavior of the silica particles in alcohol, water, and ammonia mixtures has to be investigated in much more detail. Also, the dependence of the rate constants of hydrolysis and condensation has to be measured as a function of the reaction mixture composition. However, it seems to us that the production of monodisperse colloidal silica particles from alkoxysilanes is becoming more and more a science than an art.

ACKNOWLEDGMENTS

G. Nachtegaal and A. P. M. Kentgens are thanked for their help with the NMR measurements at the SON-NWO HF-NMR facility (University of Nijmegen, The Netherlands). We also thank W. van Maurik for performing the electron microscopy measurements and M. Terlou for his help in the image analysis.

This work was supported by the Netherlands Foundation for Chemical Research (SON) with financial aid from the Netherlands Organization for Scientific Research (NWO).

REFERENCES

1. (a) Stöber, W., Fink, A., and Bohn, E., *J. Colloid Interface Sci.* **26,** 62 (1968); (b) Kolbe, G., Dissertation, Jena, 1956.
2. Van Helden, A. K., Jansen, J. W., and Vrij, A., *J. Colloid Interface Sci.* **81,** 354 (1981).
3. Bogush, G. H., Tracy, M. A., and Zukoski, C. F., IV, *J. Non-Cryst. Solids* **104,** 95 (1988).
4. Philipse, A. P., *Colloid Polym. Sci.* **266,** 1174 (1988).
5. Van Blaaderen, A., and Vrij, A., "Synthesis and Characterization of Colloidal Model Particles Made from (Organo)-Alkoxysilanes," paper presented at R. K. Iler Memorial Symposium, Washington, DC, August 1990; to appear in "Colloid Chemistry of Silica" (H. Bergna, Ed.), Advances in Chemistry Series No. 234.
6. Byers, C. H., Harris, M. T., and Williams, D. F., *Ind. Eng. Chem. Res.* **26,** 1923 (1987).
7. Harris, M. T., Brunson, R. R., and Byers, C. H., *J. Non-Cryst. Solids* **121,** 397, (1990).
8. Matsoukas, T., and Gulari, E., *J. Colloid Interface Sci.* **124,** 252 (1988).
9. Matsoukas, T., and Gulari, E., *J. Colloid Interface Sci.* **132,** 13 (1989).
10. Matsoukas, T., and Gulari, E., *J. Colloid Interface Sci.* **145,** 557 (1991).
11. Bogush, G., and Zukoski, C., "The Colloid Chemistry of Graving Silica Spheres" (Ceramic Microstructures '86). Plenum, New York, 1987. Some of these results are also presented in Brinker, C. J., and Scherer, G. W., "Sol–Gel Science," 1st ed., pp. 199–203. Academic Press, Boston, 1990.

12. Kim, S., and Zukoski, C. F., *J. Colloid Interface Sci.* **139,** 198 (1990).
13. Bogush, G. H., and Zukoski, C. F., IV, *J. Colloid Interface Sci.* **142,** 1 (1991).
14. Bogush, G. H., and Zukoski, C. F., IV, *J. Colloid Interface Sci.* **142,** 17 (1991).
15. Bailey, J. K., and Mecartney, M. L. J., *in* "Better Ceramics Through Chemistry III" (C. J. Brinker, D. E. Clark, and D. R. Ulrich, Eds.), pp. 367–372. Mat. Res. Soc., Pittsburgh, 1988.
16. Bailey, J. K., and Mecartney, M. L., *Colloids Surf.* **63,** 151 (1992).
17. Van Blaaderen, A., and Kentgens, A. P. M., *J. Non-Cryst. Solids,* in press.
18. Bradford, E. B., Vanderhoff, J. W., and Alfrey, T., Jr., *J. Colloid Interface Sci.* **11,** 135 (1956).
19. Overbeek, J. Th. G., *Adv. Colloid Interface Sci.* **15,** 251 (1982).
20. Kerker, M., "Scattering of Light and Other Electromagnetic Radiation." Academic Press, New York, 1969.
21. Philipse, A. P., and Vrij, A., *J. Chem. Phys.* **87,** 5634 (1987).
22. Dhont, J. K. G., Dissertation, University of Utrecht, 1985.
23. Weast, R. C. (Ed.), "Handbook of Chemistry and Physics," 56th ed. Chem. Rubber Pub. Co., Cleveland, 1976.
24. Dhont, J. K. G., Harder, G., Van der Werf, C. G., Van Blaaderen, A., Lekkerkerker, H. N. W., Breiner, H., and Moser, H. O., to be published.
25. Dhont, J. K. G., Smits, C., and Lekkerkerker, H. N. W., *J. Colloid Interface Sci.,* in press.
26. de Rooy, N., Dissertation, University of Utrecht, 1979.
27. Verwey, E. J. W., and Overbeek, J. Th. G., "Theory of the Stability of Lyophobic Colloids." Elsevier, New York, 1948.
28. Van Blaaderen, A., and Vrij, A., *J. Colloid Interface Sci.,* in press.